THE EFFECT OF BIAXIAL ORIENTATION PROCESSING CONDITIONS

ON IMMISCIBLE POLYMER BLENDED SHEET

Jennifer K. Lynch, Ph.D., Rutgers University
Thomas J. Nosker, Ph.D., Rutgers University
James D. Idol, Ph.D., Rutgers University

Abstract

The effect of simultaneous biaxial orientation processing conditions upon the thermal and morphological properties of PS/HDPE and PC/PMMA immiscible polymer blended sheet samples is investigated by singly varying the draw rate and draw range. Bi-component blends were melt-blended by twin screw extrusion at composition ratios selected to result in dual phase, co-continuous structures. Findings from this work will be applied to a future study of these blended sheet samples as gas separation membranes.

Introduction

Biaxial orientation is the act of stretching a sheet specimen in the transverse and longitudinal directions, simultaneously or sequentially, in a controlled manner. This type of processing is utilized to enhance certain properties of the material. For example, efficient gas separation membranes must be thin and semi-permeable. Controlled stretching of an extruded film will generate openings in the impermeable surface of the film that result from extrusion and increase the size and number of apertures and paths for molecular migration normal to the film surface. However, orientation of a specific sheet sample is limited by the generation of harmful pinholes in the stretched membrane. Successful stretching of an extruded film is dependent upon the orientation processing conditions. The orientation processing conditions are qualified by draw rate, draw range, and temperature.

The objective of this work was to determine the effect of biaxial orientation processing conditions on the thermal and morphological properties of immiscible polymer blended (IMPB) extruded sheet. By singly varying draw rate and draw range at the optimized temperature for each blend, the effect of biaxial orientation processing conditions is resolved. IMPB sheet specimens were simultaneously biaxially oriented in order to improve gas separation properties and to decrease sheet thickness in an offline orientation machine.

Materials

Thermoplastic polymers, high density polyethylene (HDPE), polystyrene (PS), polymethylmethacrylate (PMMA), and polycarbonate (PC), were selected to form bi-component IMPB sheet investigated in this study. Extrusion of the IMPB sheet was followed by simultaneous biaxial orientation. An amorphous/semi-crystalline blend of 35/65 % PS/HDPE and an amorphous/amorphous blend of 76/24 % PC/PMMA IMPB sheet samples were investigated. Both blends did not contain compatibilizers.

The bi-component blends were mechanically mixed followed by melt-blending utilizing twin screw extrusion. The composition ratio of each blend was selected to yield co-continuous, dual phase morphologies according to a semi-empirical relationship between the viscosity and volume fraction ratio at the processing temperature and shear rate of interest.[1] Immiscibility of the two blends is required so that there is no molecular interfacial bonding of the phases as they are melt-processed.

Experimental Procedures

A Leistritz inter-meshing, or co-rotating, twin screw extruder with compounding elements and a sheet die attachment was utilized to extrude IMPB sheet composed of PS/HDPE and PC/PMMA at a processing temperature of approximately 200 ℃.

Specimen preparation involved cutting out a 12.5 cm square area from the central region of the extruded PS/HDPE and PC/PMMA sheet and drawing grid lines on the surface of each specimen at increments of 0.6 cm. Grid lines were drawn in order to determine the uniformity of the orientation. The prepared samples were simultaneously biaxially oriented utilizing an offline orientation machine, custom designed by Inovent, Inc. of Cleveland, OH. The machine's processing conditions include Temperature (38 – 177 ℃), Draw Rate (2.5 – 25 cm/min), and Draw Range (10 – 50 cm).

[1] Jordhamo, G.M., Manson, J.A., and Sperling, L.H., Polymer Engineering and Science, **26** (8), 1986.

Specimens were biaxially oriented simultaneously from an initial 10 cm square area to the desired draw range at a specified draw rate and temperature. Prior to orientation, the appropriate temperature was established for each blend. The processing temperatures were 132 ℃ and 156 ℃ for the PS/HDPE and PC/PMMA blends, respectively. Two draw rates and two draw ranges were selected and singly varied at the optimized temperature for each blend. The selected draw rates were 10 and 25 cm/min for both blends. The original range was 10 x 10 cm, referred to as a 10 cm range. Following this labeling system, the selected draw ranges were 20 and 30 cm for the PS/HDPE blend, and 20 and 25 cm for the PC/PMMA blend. Each sample, PS/HDPE and PC/PMMA, is comprised of oriented specimens labeled 1-4 and the unoriented specimen labeled 'original'.

Thickness measurements of the IMPB sheets were performed using a Positector 6000 thickness gage utilizing Eddy current techniques before and after biaxial orientation. Prior to orientation, measurements were taken in each box defined by the drawn grid lines. Post orientation, sheet thickness measurements were taken in each grid box in the sheet's central region defined by the square area inside a 2.5 cm perimeter from all edges.

The morphology of the PS/HDPE and PC/PMMA samples was investigated using a Leo-Zeiss DSM 982 Gemini Field Emission Scanning Electron microscope. All prepared specimens were fractured at liquid nitrogen temperatures, and the fracture surface was goad coated for increased resolution during viewing. Specimens were viewed parallel and perpendicular to the extrusion axis.

Thermal properties were determined using a TA Instruments Q 1000 Differential Scanning Calorimeter in modulated mode (MDSC) under an atmosphere of dry nitrogen. Specimens ranging between 7–10 mg of the PS/HDPE and PC/PMMA samples were encapsulated in standard aluminum pans and sealed by crimping. All MDSC scans were conducted at 3 °C/minute over 40-200 °C while simultaneously modulating at +/- 1.3 °C every 40 seconds. All specimens were heated, cooled, and reheated over the aforementioned temperature program.

Results

A two-factor, two-level analysis of the mean thickness of IMPB sheets, with respect to draw rate and draw range is presented for PS/HDPE and PC/PMMA blends in Tables 1 and 2, respectively. The average thickness of the original specimens was 411 μm and 739 μm for the PS/HDPE and PC/PMMA blends, respectively. Post biaxial orientation, the average sheet thicknesses decreased on average by 89 % for the PS/HDPE blend and by 79 % for the PC/PMMA blend. The greatest decrease in thickness corresponds to specimens stretched to the larger draw range, as expected.

Across all orientation parameters, the thickness standard deviation is consistent and low for the PS/HDPE blend but is higher and less consistent for the PC/PMMA blend. For the PC/PMMA blend, the grid lines remained uniform post orientation, however, the specimen thickness varied from the center, where it was thinner and slightly transparent, to the outer perimeter, where it was thicker and remained opaque. The thickness standard deviation would decrease for the PC/PMMA sample, if measurements were taken within a slightly smaller central region.

The morphology of the PS/HDPE sample is presented in the SEM micrographs of Figure 1 for the original sheet and the four oriented sheet specimens. The view is parallel to the sheet extrusion axis at 30K magnification with a 1 μm scale. Analysis of PS/HDPE oriented sheet specimens shows that the orientation processing parameters do not seem to affect the inter-domain gap spacing between the PS and HDPE phases. The inter-domain gap spacing remains in the range of 70–170 nm for the entire PS/HDPE sample. This result is unexpected but may be due to high mechanical bonding at the interface between the PS and HDPE phases or due to the SEM specimen preparation. PS and HDPE domains are on the order of 200–1000 nm.

The morphology of the PC/PMMA sample is presented in the SEM micrographs of Figure 2 for the original sheet and the four oriented sheet specimens. The view is parallel to the sheet extrusion axis at 10K magnification with a 2 μm scale. Analysis of PC/PMMA sheet specimens shows that the PC and PMMA phases form an alternating stacking structure, the inter-domain gap spacing between the PC and PMMA phases is undetectable, the oriented specimens are less tightly packed than the un-oriented specimen, small holes less than 100 nm are dispersed throughout all oriented specimens, and that large holes on the order of 1000 nm were formed in the specimens oriented to the largest draw range creating an open, honeycomb-like structure.

Thermal analysis results are presented in Figures 3–7. Figure 3 shows thermal properties determined for PS/HDPE original and oriented specimens. In the initial scan, the HDPE phase melting temperature increases from 127 ℃ for the original specimen to 130 ℃ for all of the oriented specimens suggesting an increase in crystallinity with biaxial orientation. During the reheat, the HDPE melting temperature is constant around 130 ℃ across the entire sample. For the initial and reheat, the PS glass transition temperature (Tg) remains constant at 103 ℃ for the entire sample. Figure 4 depicts the heat of fusion for PS/HDPE sample corresponding to the HDPE melting/crystallization transition. During the initial heat, the original specimen's heat of fusion is 109 J/g while the oriented specimens have heats of fusion ranging from 125–131 J/g. Thus, there is an increase in the crystallinity of the HDPE phase in the PS/HDPE sheet due to biaxial

orientation. As the previous thermal history is erased, the heat of fusion is relatively constant during the cool and reheat scans. Figure 5 presents the derivative of the reversing heat flow for the initial DSC scans for the PC/PMMA sample. It is evident from the original specimen's initial heat scan that the orientation imparted by the extrusion process alone has affected the temperature transitions causing four distinct temperature transitions rather than just two Tgs corresponding to each amorphous polymer component. Further orientation in specimens 1–4 follow this trend suggesting the release of stored strain energy upon heating due to stresses imparted in the material during biaxial orientation and the possibility of induced crystallinity in the polycarbonate phase as a result of biaxial orientation. Induced crystallinity of PC due to orientation is supported in the literature due to fiber drawing, solvent induced crystallinity in conjunction with drawing, and drawing in the presence of super critical carbon dioxide but must be investigated further for the presented case of biaxial orientation. Figure 6 presents the four thermal transitions from the derivative of the reversing heat flow curves in Figure 5 for the PC/PMMA sample. One may assume that T1 corresponds to the Tg of the PMMA phase, however, it is not clear which transition temperature corresponds with the Tg of the PC phase. Note that specimens 3 and 4 do not have a T3 transition. Figure 7 depicts the reheat derivative of the reversing heat flow DSC scan for the PC/PMMA sample, in which two distinct Tgs exist at 112 ℃ and 146 ℃ corresponding to PMMA and PC, respectively. Figure 7 indicates all stored strain energy and any induced crystallinity in the PC phase due to biaxial orientation disappears after the initial heat.

Conclusion

Biaxial orientation parameters may be tailored to produce the desired film thickness, degree of orientation, and degree of crystallinity of an IMPB membrane. This investigation of the effect of biaxial orientation processing conditions on IMPB sheet is a preliminary study that is a stepping stone to further research. The primary outcome is that biaxial orientation of PS/HDPE and PC/PMMA IMPB membranes produces potential candidates for gas separation membranes.

Future work will include gas diffusion or permeability studies of multiple gases through these IMPB membranes, Raman spectroscopy to determine the effect of orientation on the crystallinity of HDPE in the PS/HDPE blend and PC in the PC/PMMA blend, further thermal analysis to verify the four transitions of the PC/PMMA sample, further SEM analysis adopting different sample preparation techniques, and a simple determination of the degree of orientation by measuring the shrinkage of oriented specimens upon reheating post orientation because this shrinkage is directly proportional to the degree of orientation in the sheet.

Acknowledgements

Table 1.   Oriented PS/HDPE immiscible polymer blended sheet orientation parameters and results

Specimen	Draw Rate (cm/min)	Draw Range (cm)	Temperature (℃)	Thickness (μm)	STD Thickness (μm)	Area (cm^2)
Original	None	10		411	9	100
1	10	20	132	72	19	400
2	10	30	132	33	19	900
3	25	20	132	44	19	400
4	25	30	132	34	21	900

Table 2.   Oriented PC/PMMA immiscible polymer blended sheet orientation parameters and results

Specimen	Draw Rate (cm/min)	Draw Range (cm)	Temperature (℃)	Thickness (μm)	STD Thickness (μm)	Area (cm^2)
Original	None	10		739	7	100
1	10	20	156	208	62	400
2	10	25	156	105	61	625
3	25	20	156	174	93	400
4	25	25	156	123	57	625

PS-HDPE
Parallel to x
at 30 K

20 cm

Original

10 cm/min

25 cm/min

30 cm
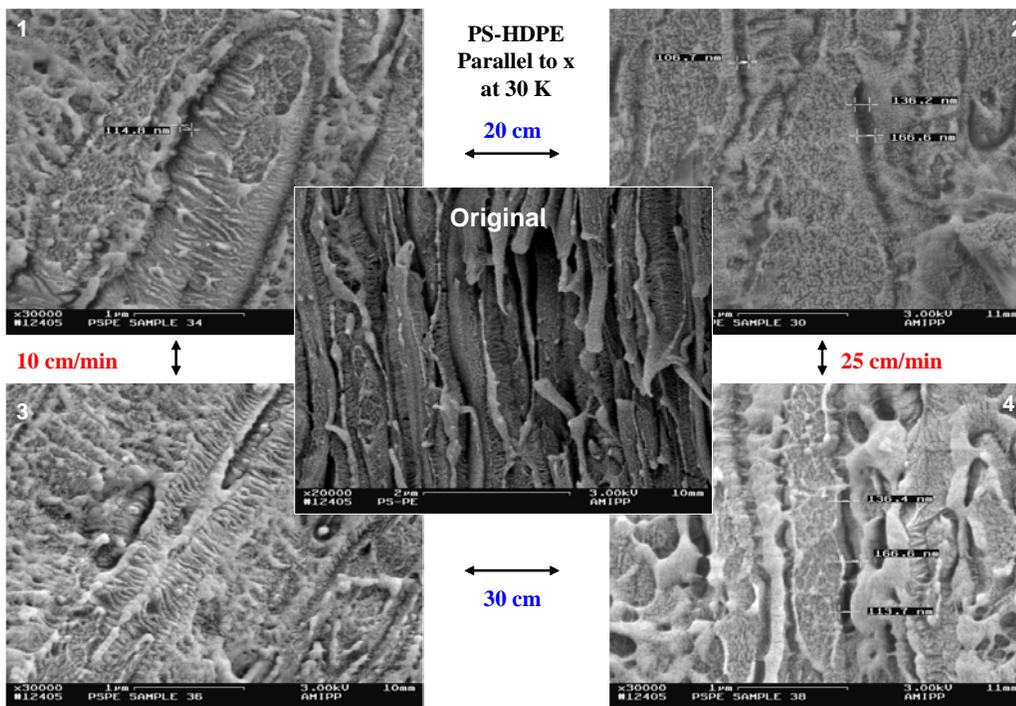
Figure 1. SEM micrographs of PS/HDPE IMPB original and oriented sheet specimens

PC/PMMA
Parallel to x
at 10 K

20 cm

Original

10 cm/min

25 cm/min

25 cm
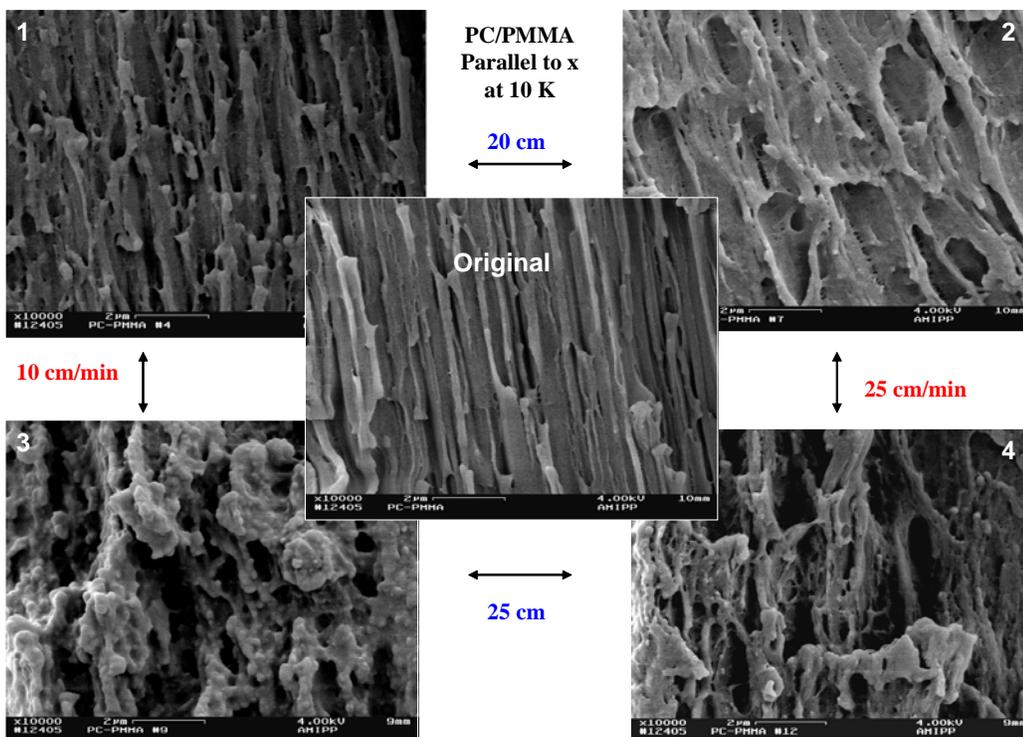
Figure 2. SEM micrographs of PC/PMMA IMPB original and oriented sheet specimens

PS/HDPE
Thermal Properties - Total Heat Flow
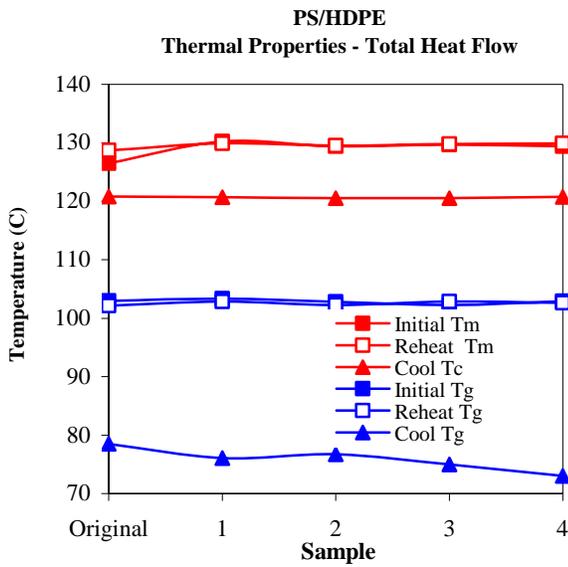
Figure 3. Thermal properties for PS/HDPE IMPB original and oriented sheet specimens. Red lines correspond to the melting and crystallization of the HDPE phase, and blue lines correspond to the glass transition of the PS phase.

PS/HDPE
Heat of Fusion - Total Heat Flow
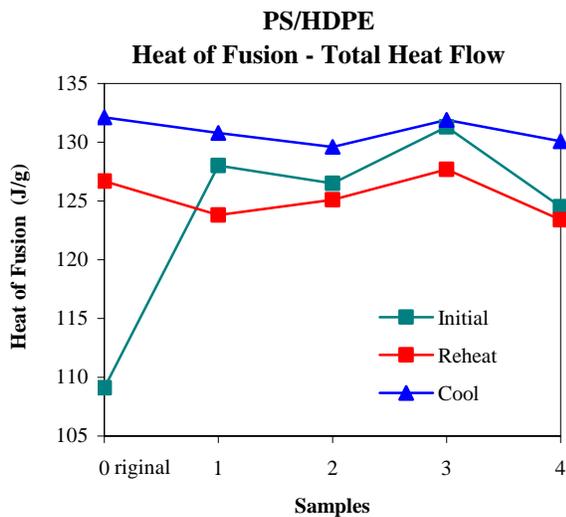
Figure 4. Heat of fusion for PS/HDPE IMPB original and oriented sheet specimens corresponding to the HDPE melting/crystallization transition

PC/PMMA
Intial Heat - Derivative Reversing Heat Flow
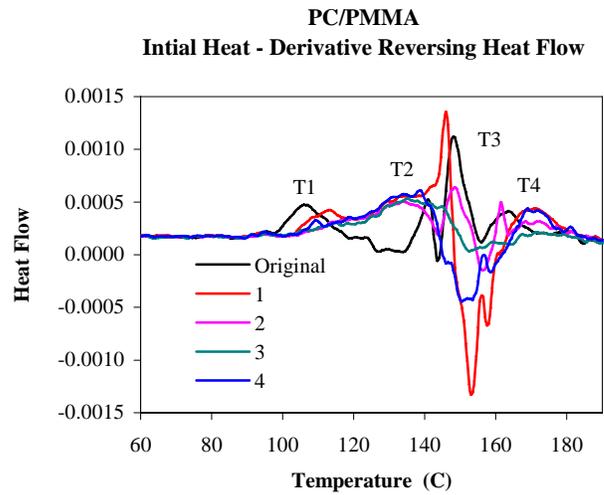
Figure 5. Total heat flow of the initial MDSC scan for PC/PMMA IMPB original and oriented sheet specimens

PC/PMMA
Thermal Transitions
Initial Heat - Derivative Reversing Heat Flow
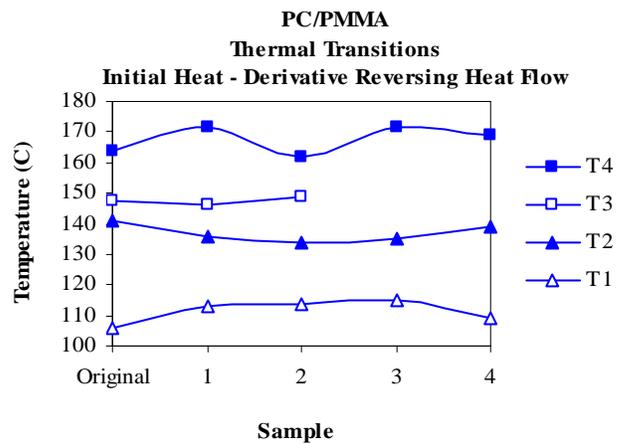
Figure 6. Thermal transitions from the derivative of the reversing initial heat flow curves for PC/PMMA IMPB original and oriented sheet specimens

PC/PMMA
Reheat - Derivative Reversing Heat Flow
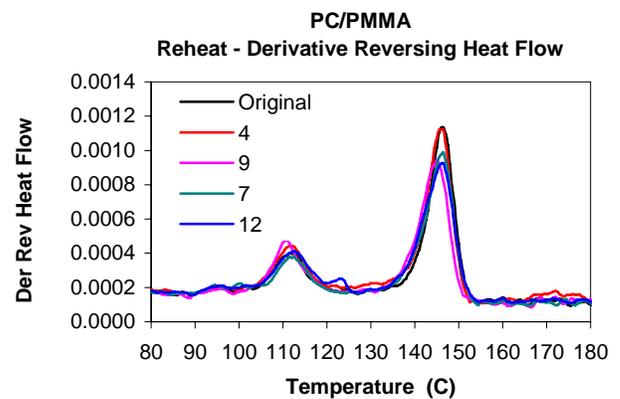
Figure 7. Derivative of the reversing heat flow of the reheat MDSC scan for PC/PMMA IMPB original and oriented sheet specimens